Observational Cosmology Journal Club

March 5, 2018, Taira Oogi

[1] LoCuSS: pre-processing in galaxy groups falling into massive galaxy clusters at z=0.2
M. Bianconi et al.; arXiv:1710.04230

[2] GASP IX. Jellyfish galaxies in phase-space: an orbital study of intense ram-pressure stripping in clusters
Yara. L. Jaffe et al.; arXiv:1802.07297

[3] On the (fast) quenching of (young) low-mass galaxies to z~0.6
New spotlights on environment lead role
Thibaud Moutard et al.; arXiv:1802.07628

[1] LoCuSS: pre-processing in galaxy groups falling into clusters

Haines et al. 2015

Radial population gradient of cluster galaxies: the fraction of star-forming galaxies remains well below field values even at 3 r_200.

Suggestion:
the presence of environmental effects accelerating the consumption of the gas reservoir prior to the settling of the galaxy into the cluster potential, pre-processing.

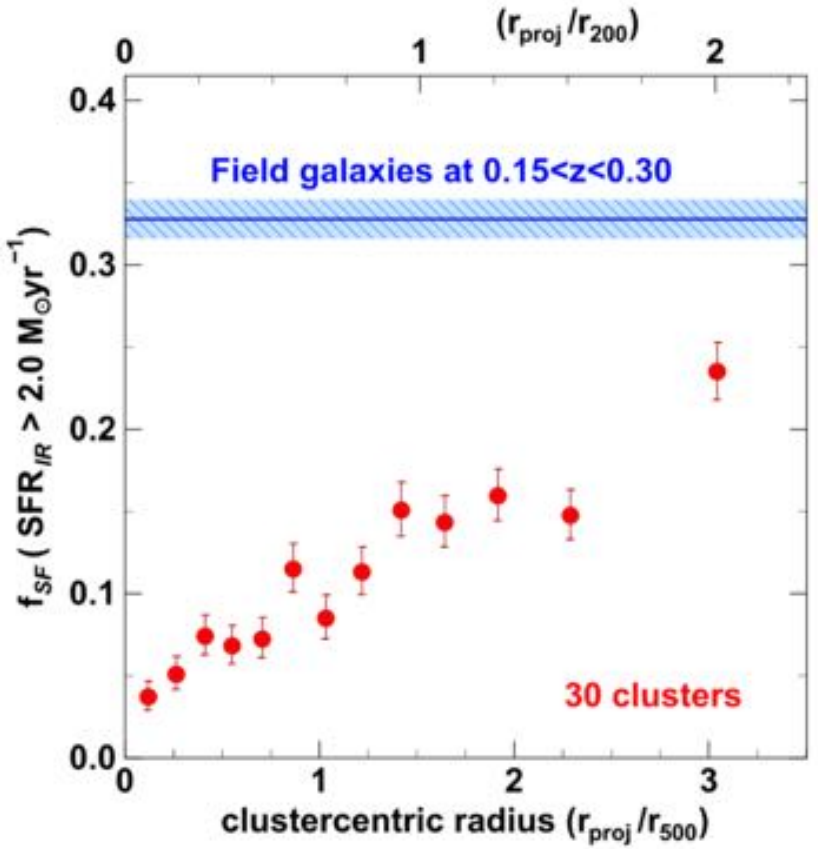

Figure 2. Radial population gradients for MIR-selected star-forming galaxies from our stacked sample of 30 clusters. Red symbols show the fraction of massive ($\mathcal{M} > 2.0 \times 10^{10}\,M_\odot$) cluster galaxies with obscured star formation at rates $SFR_{IR} > 2.0\,M_\odot\ yr^{-1}$ as a function of projected cluster-centric radius (r_{proj}/r_{500}). The error bars indicate the uncertainties derived from binomial statistics calculated using the formulae of Gehrels (1986). Each radial bin contains 400 cluster galaxies. The blue horizontal line indicates the corresponding fraction of field galaxies ($\mathcal{M} > 2.0 \times 10^{10}\,M_\odot$; $0.15 < z < 0.30$) with $SFR_{IR} > 2.0\,M_\odot\ yr^{-1}$ and its 1σ confidence limits (shaded region).

[1] LoCuSS: pre-processing in galaxy groups falling into clusters

The Local Cluster Substructure survey (LoCuSS)

Haines et al. 2017

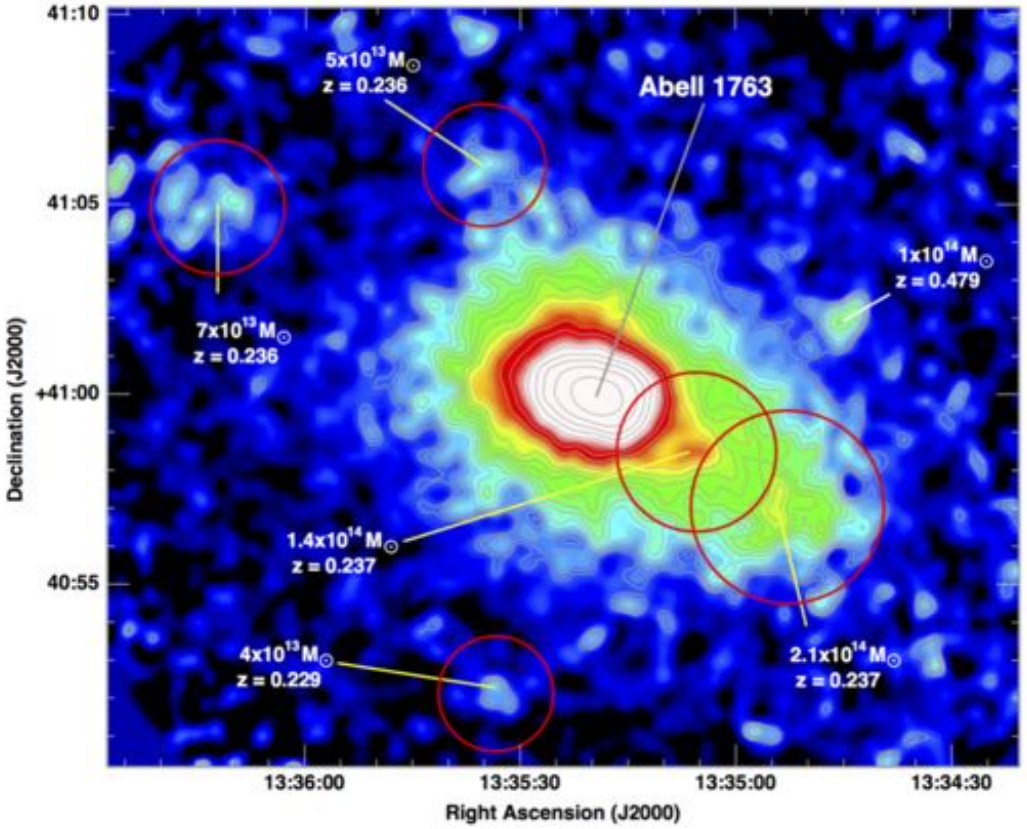

Figure 2. Extended X-ray emission from Abell 1763. All spectroscopically confirmed X-ray groups are indicated and labelled by their redshift and estimated M_{200} value. Those groups which are infalling into Abell 1763 are marked by red circles of diameter r_{200}.

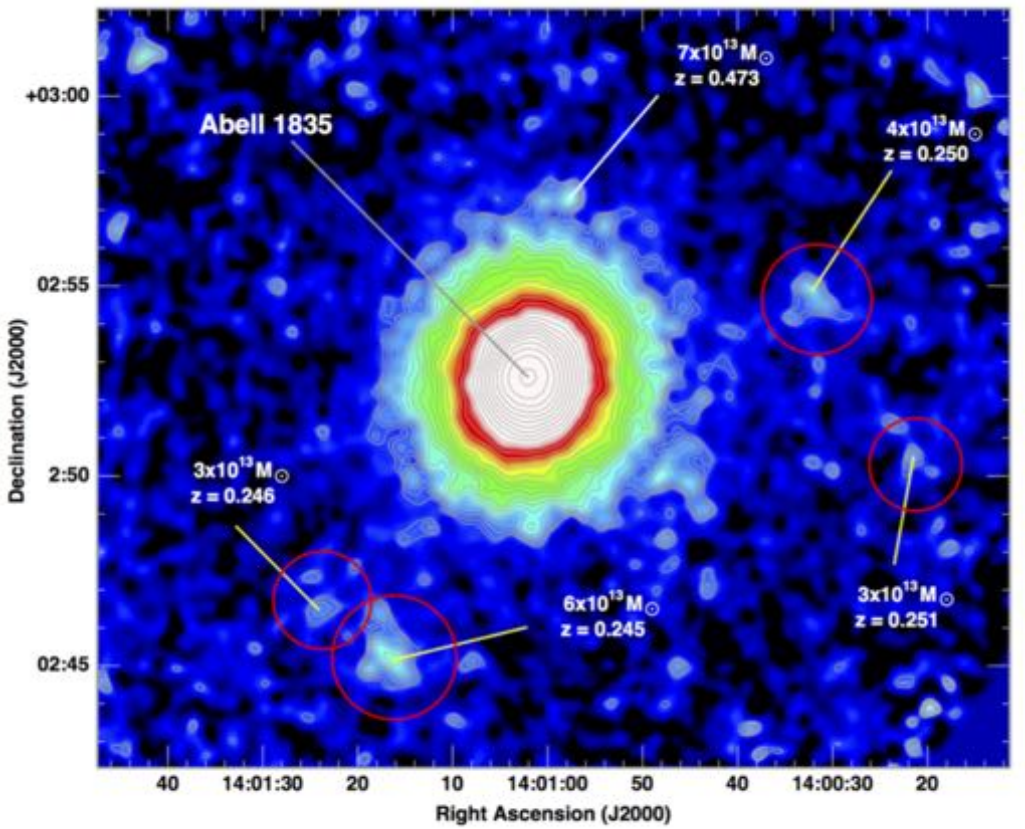

Figure 3. Extended X-ray emission from Abell 1835. All spectroscopically confirmed X-ray groups are indicated and labelled by their redshift and estimated M_{200} value. Those groups which are infalling into Abell 1835 are marked by red circles of diameter r_{200}.

They present a study of a new sample of recently discovered infalling groups (Haines et al. 2017), focusing in particular on the star-formation properties of the massive galaxies within them.

[1] LoCuSS: pre-processing in galaxy groups falling into clusters

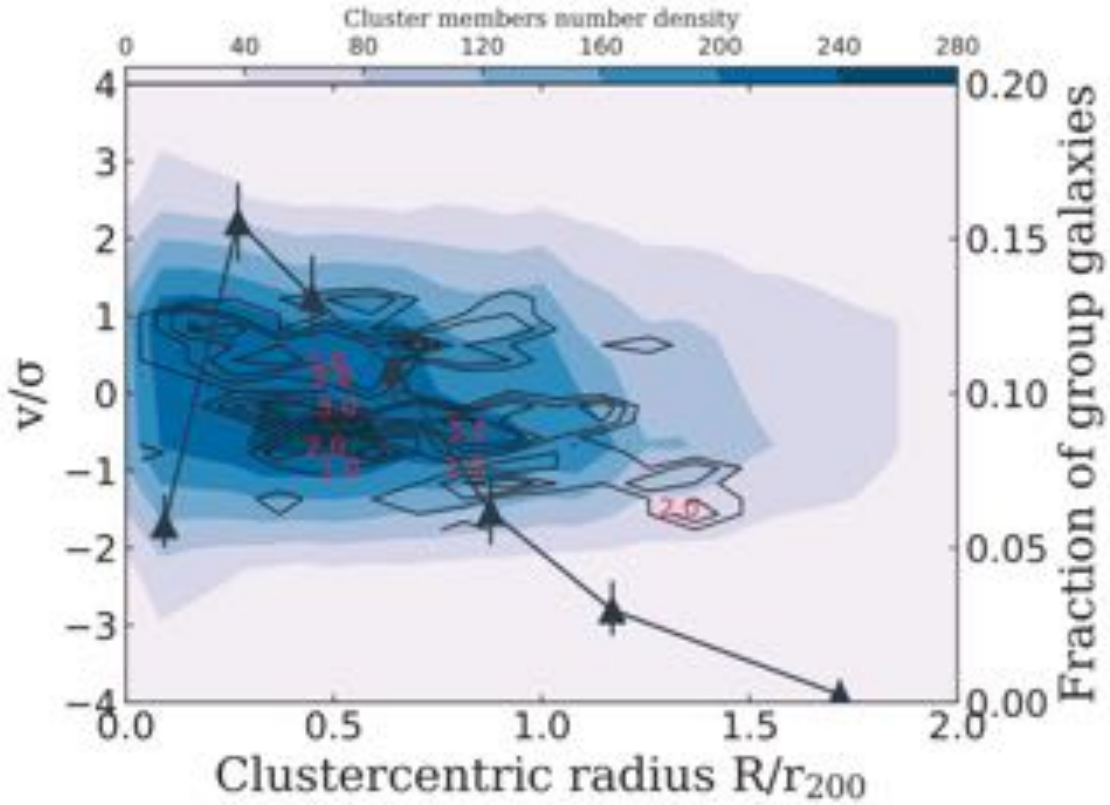

Figure 1. Density map of the line-of-sight peculiar velocity (in units of σ) versus clustercentric radius (in units of r_{200}) of cluster members. Superimposed black contours are labelled in red with the number density of the 34 infalling group members. Filled grey triangles show the fraction of group members with respect to cluster members, as a function of clustercentric radius. The error bars (at 1σ) are computed from binomial statistics following Gehrels (1986).

[1] LoCuSS: pre-processing in galaxy groups falling into clusters

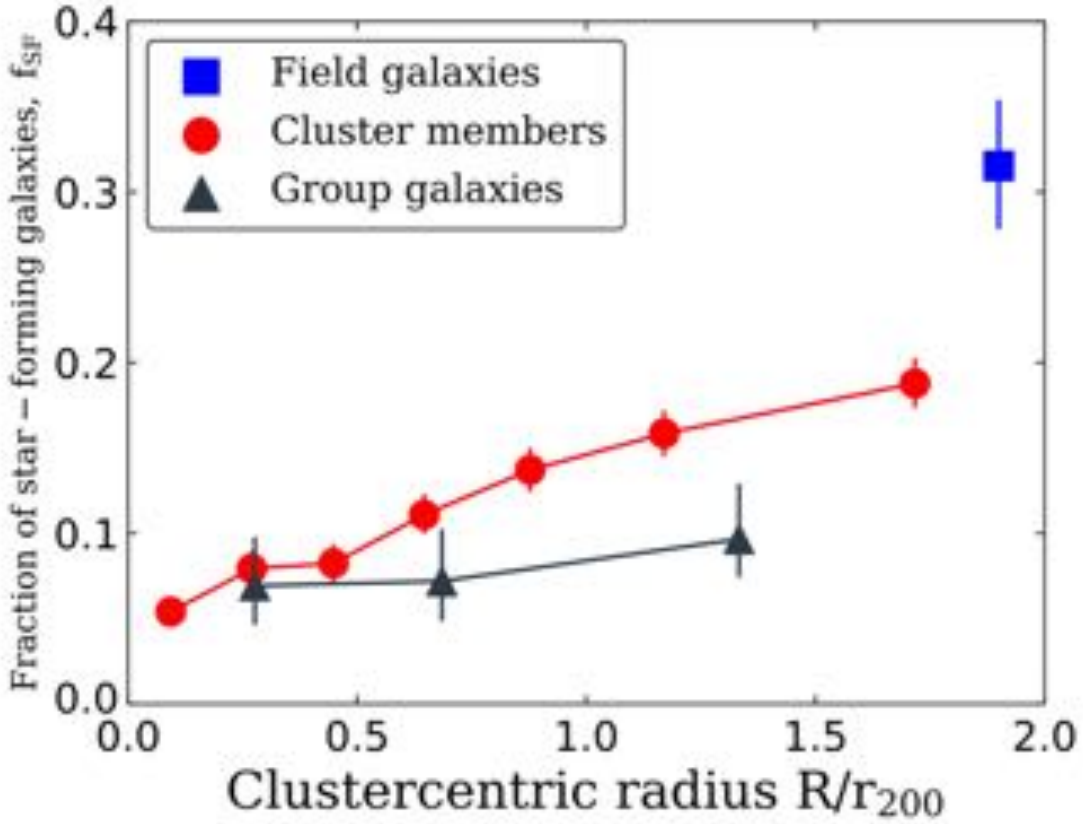

Figure 2. Fraction of massive ($M_* > 2 \times 10^{10}\,M_\odot$) star-forming (SFR $> 2\,M_\odot\,yr^{-1}$) galaxies, f_{sf}, plotted with respect to projected clustercentric distance in units of r_{200}. Galaxies in LoCuSS clusters and infalling groups are plotted as filled red circles and grey triangles, respectively. The f_{sf} of field galaxies is plotted as filled blue squares at an arbitrary radius.The error bars (at 1σ) are computed from binomial statistics following Gehrels (1986). Each radial bin contains on average 723 cluster and 125 group galaxies, respectively.

Conclusion: star-formation quenching is effective in galaxy groups.

[2] GASP IX. Jellyfish galaxies in phase-space

Jellyfish galaxies:
Stripped galaxies with new stars tracing the stripped tails

GAs Stripping Phenomena in the galaxies in MUSE (GASP) is a new integral-field spectroscopic survey with MUSE at the VLT.

Stripping Extreme-stripping Post-stripping ?

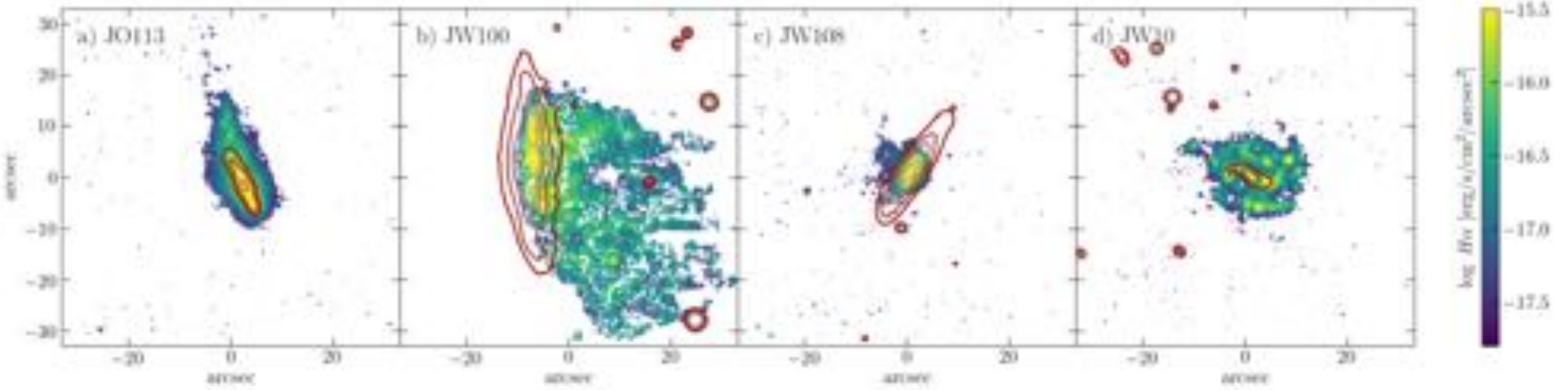

Figure 2. Hα flux emission maps (colourbar) on top of isophotes of Hα continuum in steps of 0.5 mag/arcsec^{-2} (red contours) for 4 example GASP galaxies in different stripping stages. From left to right: a) A galaxy with moderate signs of "Stripping"; b) a galaxy featuring very long gas tails indicative of "Extreme-stripping"; c) a truncated "Post-stripping" galaxy; and d) a disturbed galaxy where the physical cause of the disturbance is unclear ("?").

[2] GASP IX. Jellyfish galaxies in phase-space

- Position vs. velocity phase-space diagram
- The green “cone”: regions in phase-space where ram-pressure stripping is at play.
- Red and blue contours: the location of simulated cluster galaxies from Rhee et al. (2017).

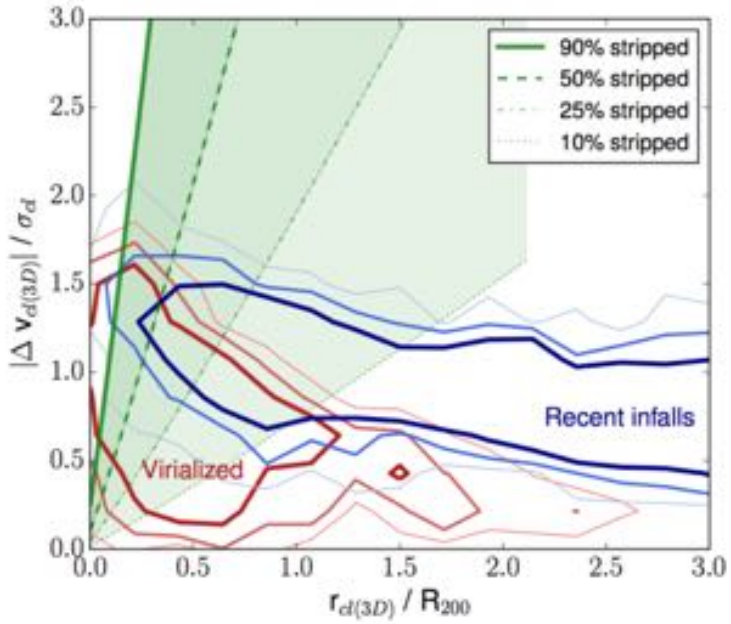

Figure 6. The position vs. velocity phase-space diagram of 15 simulated group and cluster galaxies (mass range from 0.5×10^{13} to $1 \times 10^{15} M_{\odot}$) from Rhee et al. (2017, private communication), considering multiple lines of sight, separated into “virialized” (entered the cluster > 4 Gyr ago; red contours) and “Recent infalls” (falling towards the cluster for the first time or recently entered the cluster < 2 Gyr; blue contours). A galaxy is considered to enter the cluster when it has crossed R_{200} for the first time. The contours enclose 1000, 2500, and 5000 particles from lighter to darker colours respectively. The axes have been normalized by cluster size (R_{200}) and cluster velocity dispersion (σ_{cl}) to allow the stacking of 15 simulated clusters with masses between 10^{13} and $10^{15} M_{\odot}$. The green area indicates the region where ram-pressure by the ICM is able to strip 10% (dotted line) to 90% (solid lines) of the total gas mass of an low-mass galaxy (model galaxy I) falling in a massive cluster (model cluster B). For details see Section 3, and Tables 1 and 2.

[2] GASP IX. Jellyfish galaxies in phase-space

- Jellyfish galaxies avoid the virialized region of the cluster, and have extended distribution in contrast to all cluster galaxies.

- "Extreme-stripping" are all located within $\mathbf{0.5}\ R_{200}$ and many are at $|\Delta v|/\sigma > 1$.
- "Stripping" are mostly located beyond $> \mathbf{0.5}\ R_{200}$.
- "Post-stripping" are near the center of the cluster.

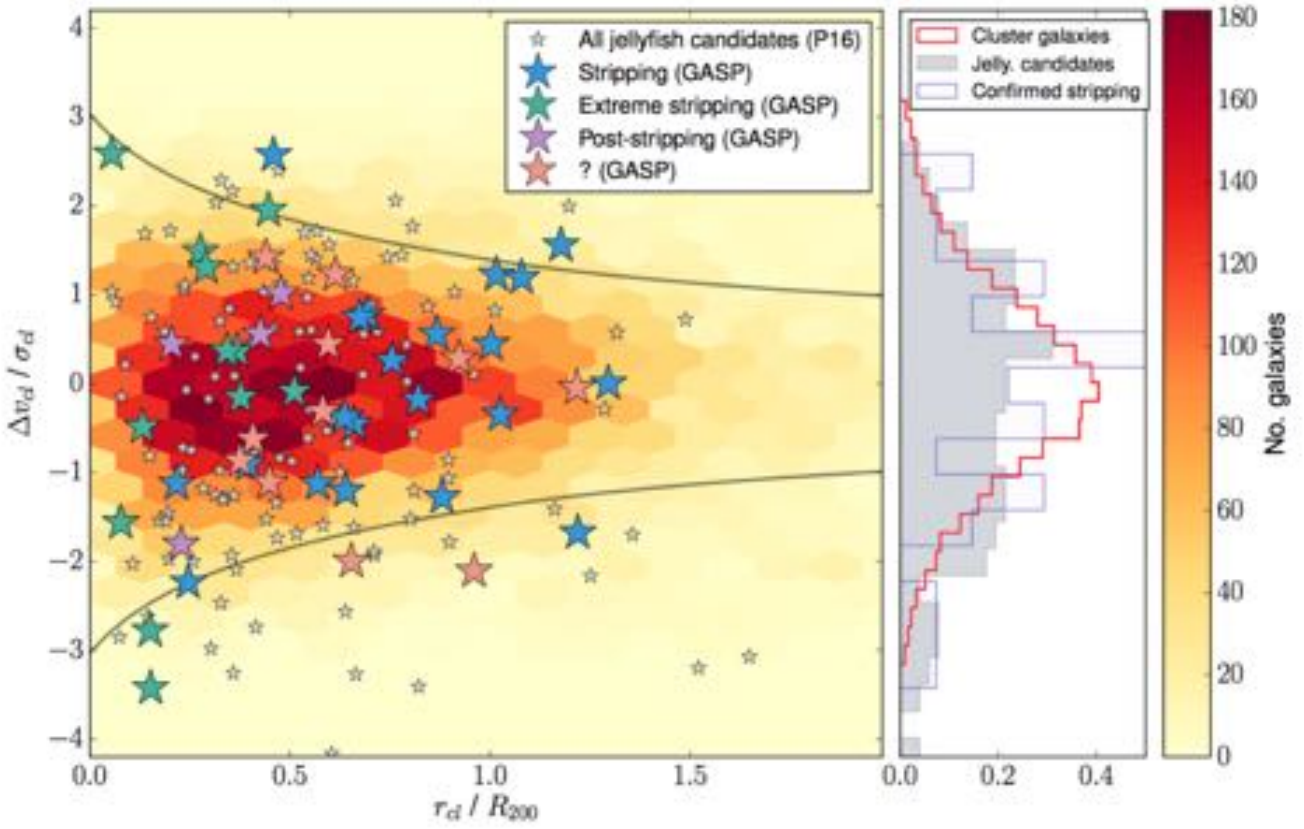

Figure 7. The location in projected position vs. velocity phase-space of all the jellyfish galaxy candidates from P16 (small gray stars) and the ones observed with MUSE by GASP so far (larger colored stars), separated by stripping stage as indicated. The background shows the distribution of all WINGS/OmegaWINGS clusters with spectroscopic completeness > 50% stacked together (orange colorbar). The gray curve corresponds to the 3D (un-projected) escape velocity in a NFW halo with concentration $c = 6$ for reference. Note that, contrary to the absolute velocities plotted in the phase-space diagram of Figure 6, the velocity axis in this plot has positive and negative values. To the right of the phase-space diagram, a plot shows the velocity distribution of the overall cluster population of galaxies (open red histogram), all the jellyfish candidates from P16 (filled grey histogram), and the galaxies observed by GASP that are confirmed stripping cases (i.e. "Stripping", "Extreme stripping", and "Post-stripping; dashed blue histogram) at $r_{cl} < R_{100}$. All histograms have been normalized to unity for comparison.

[2] GASP IX. Jellyfish galaxies in phase-space

- Extreme-stripping galaxies are high mass galaxies in both low- and high-mass clusters.
- These galaxies are inside or near the zone where ram-pressure is estimated to be most intense.

- Many stripping galaxies are low-mass galaxies in low-mass clusters located outside the high-intensity stripping zone.
- These jellyfish galaxies are possibly being affected by substructures within the cluster and clumpy ICM.

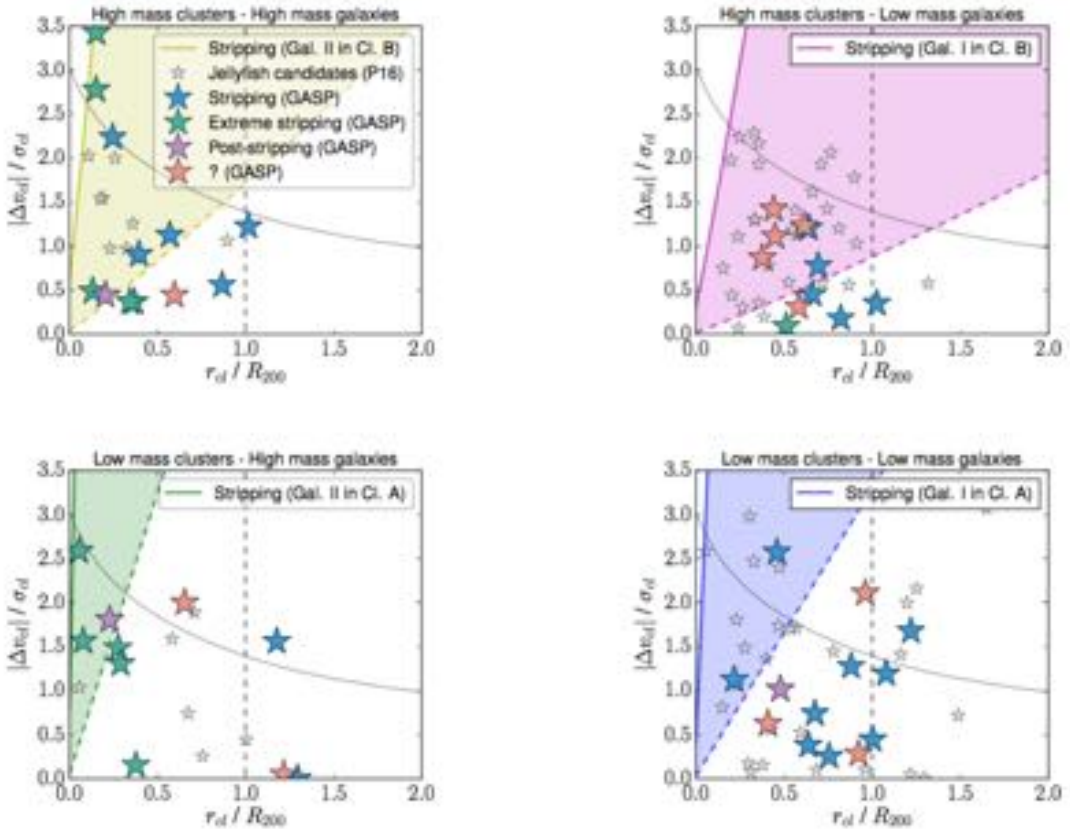

Figure 8. The location in position vs. velocity phase-space of jellyfish galaxies in high mass clusters (top panels; $\sigma_{cl} > 750km/s$) and low mass clusters (bottom panels; $\sigma_{cl} < 750km/s$)) separated in two bins of stellar mass: $> 5 \times 10^9 M_\odot$ on the left panels and $< 5 \times 10^9 M_\odot$ on the right panels. As in Figure 7, grey stars correspond to the jellyfish sample of P16 while the bigger stars are the confirmed jellyfish galaxies from GASP. Lines of different intensities of ram-pressure are indicated in each case: the dashed coloured lines indicate 10% stripping of the total gas mass, while the solid line corresponds to 90% stripping. The grey curve corresponds to the escape velocity in a NFW halo. The vertical dashed line indicates $r = R_{200}$, which is roughly the extent to which all clusters used have a high spectroscopic completeness.

[2] GASP IX. Jellyfish galaxies in phase-space

- Jellyfish galaxy population shows a dramatic increase of cluster velocity dispersion at low radii.

- Assuming that the star-forming galaxies are the progenitors of jellyfish, the steep radial cluster velocity dispersion profile of jellyfish can be explained by highly radial orbits.

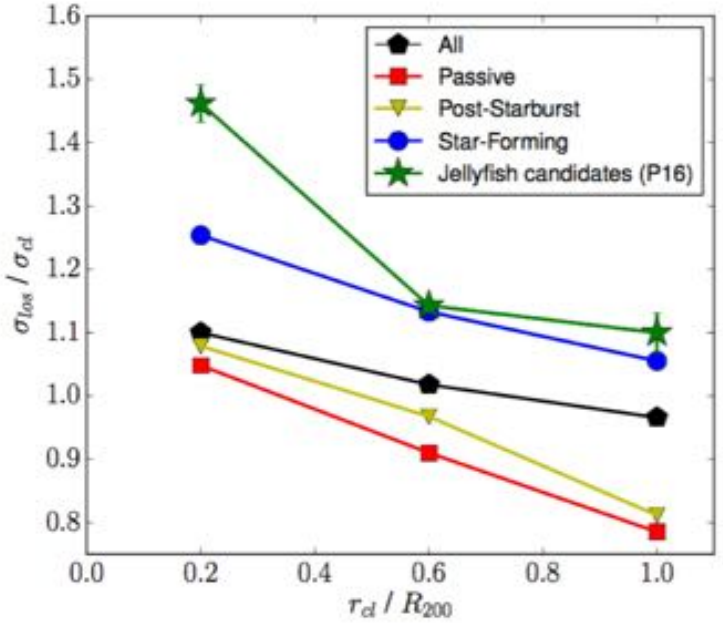

Figure 9. Line-of-sight velocity dispersion radial profiles of all the cluster jellyfish candidates from P16, and the samples of passive, star-forming, and post-starburst galaxies from Paccagnella et al. (2017), normalized by the velocity dispersion of the cluster as a function of distance from the cluster centre in units of R_{200}. The parent sample of WINGS/OmegaWINGS cluster galaxies is plotted in black for reference. We considered all candidate jellyfish (which include the confirmed cases from GASP) and did not differentiate by class to increase the number of galaxies per radial bin. Errors are jackknife standard deviations. For this plot we restricted the galaxy samples to the clusters with spectroscopic completeness > 50% and clustercentric distances $r_{cl} < R_{200}$ to minimize biases.

Conclusion: jellyfish galaxies are a population of recently accreted cluster galaxies on highly radial orbits, that are stripped via ram-pressure.

[3] On the (fast) quenching of (young) low-mass galaxies to z~0.6

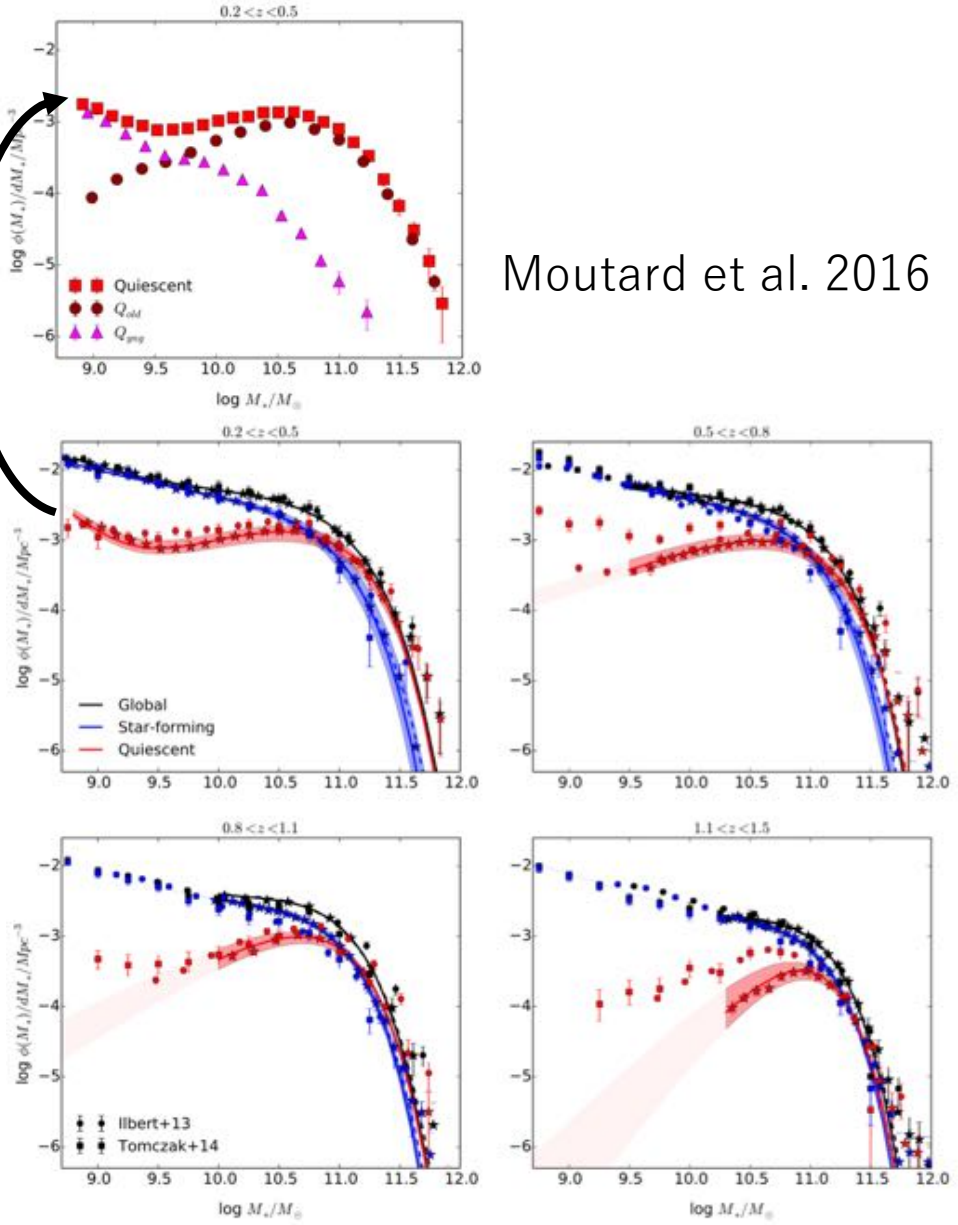

Moutard et al. 2016

- The main feature of the VIPERS Multi-Lambda Survey (VIPER-MLS) is its ability to investigate the galaxy properties as a function of environment at high redshift.
- The unique combination of area, depth and photometric multi-wavelength coverage of the VIPER-MLS.
- Covering >22 deg^2 down to $K_s < 22$, the VIPER-MLS provides a complete sample of galaxies down to stellar masses of $M_* \sim= 10^{9.4}$ M_{sun} at z<0.65 ($M_* \sim= 10^{8.8}$ M_{sun} at z<0.5) including more than 33,500 (43,000) quiescent galaxies.
- Photometric redshift with $\sigma_{\delta z/(1+z)} \leq 0.04$.

- Fast quenching channel of young low-mass galaxies

[3] On the (fast) quenching of (young) low-mass galaxies to z~0.6

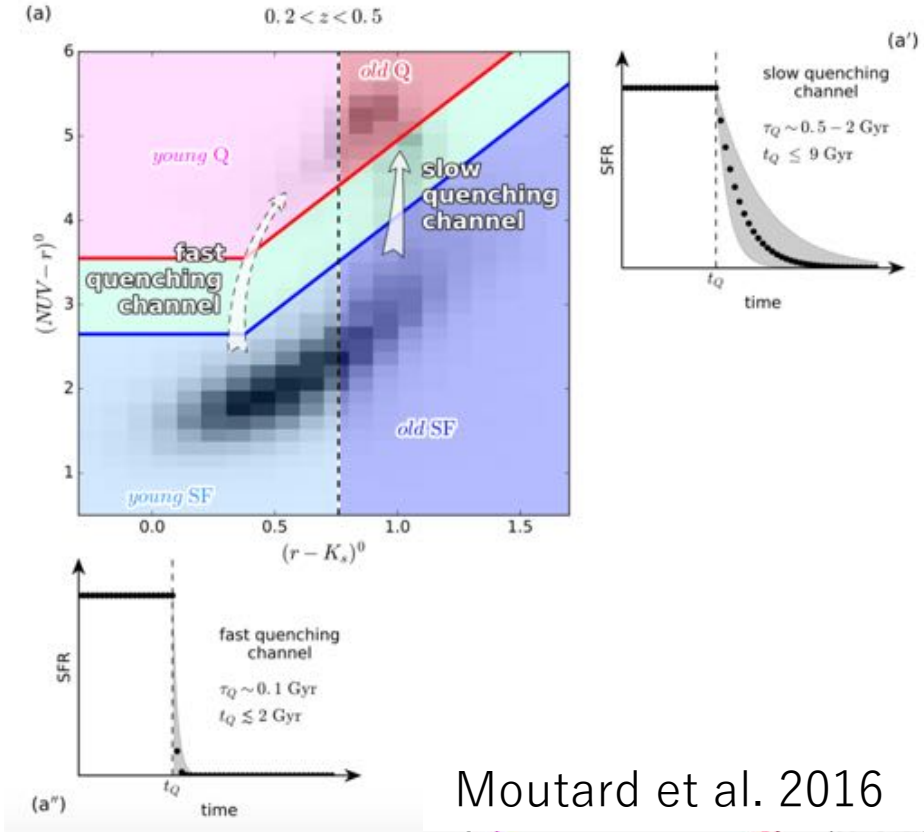

Moutard et al. 2016

Pathway of galaxies in the color—color plane

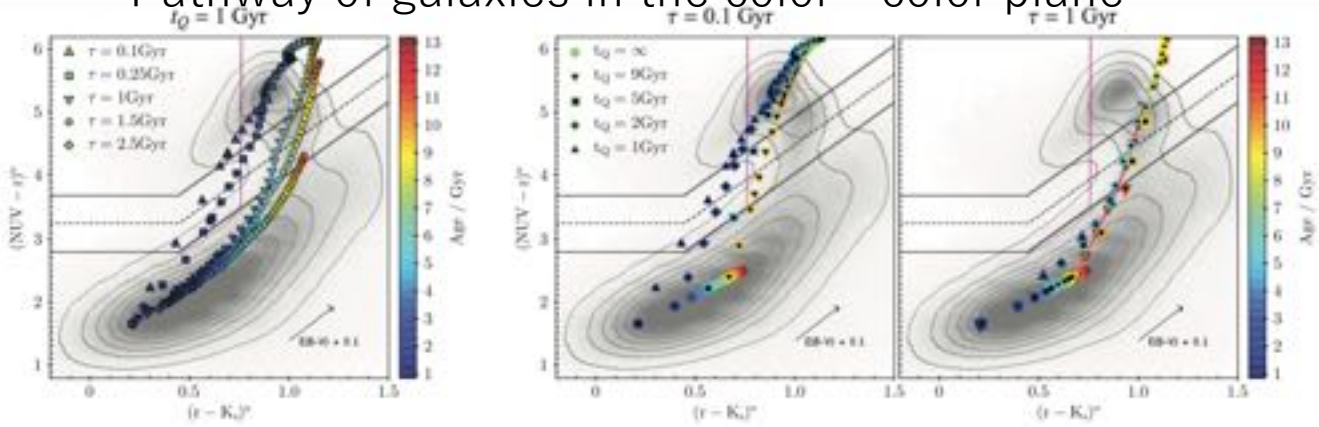

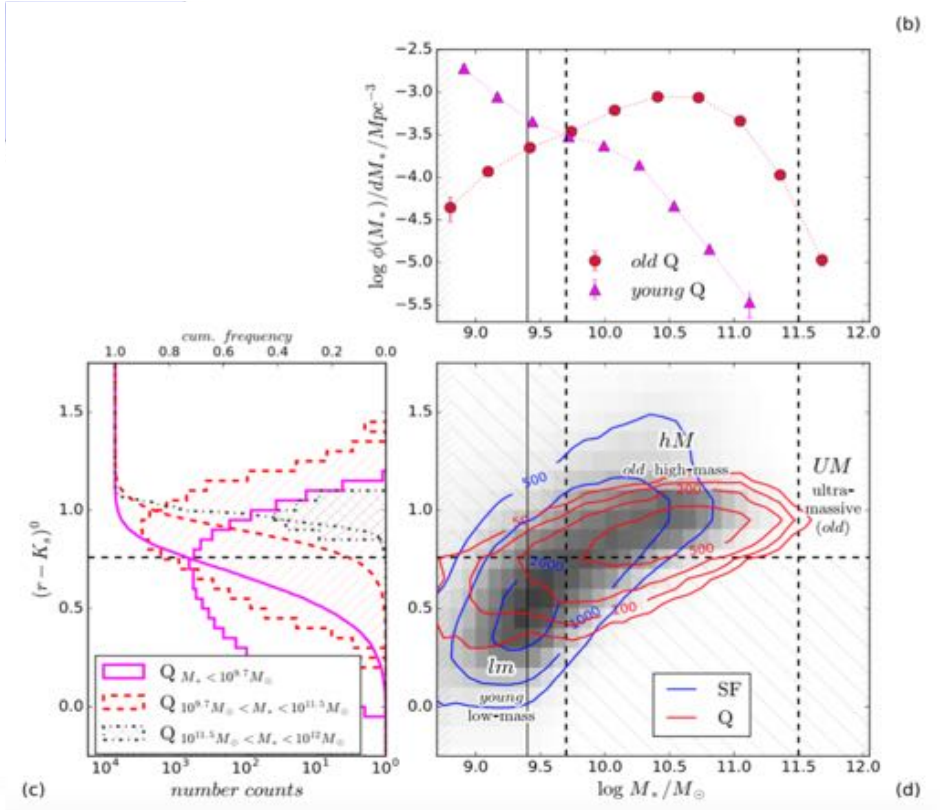

[3] On the (fast) quenching of (young) low-mass galaxies to z~0.6

The aim of this study is to highlight the role of environment in the fast quenching of low-mass galaxies.

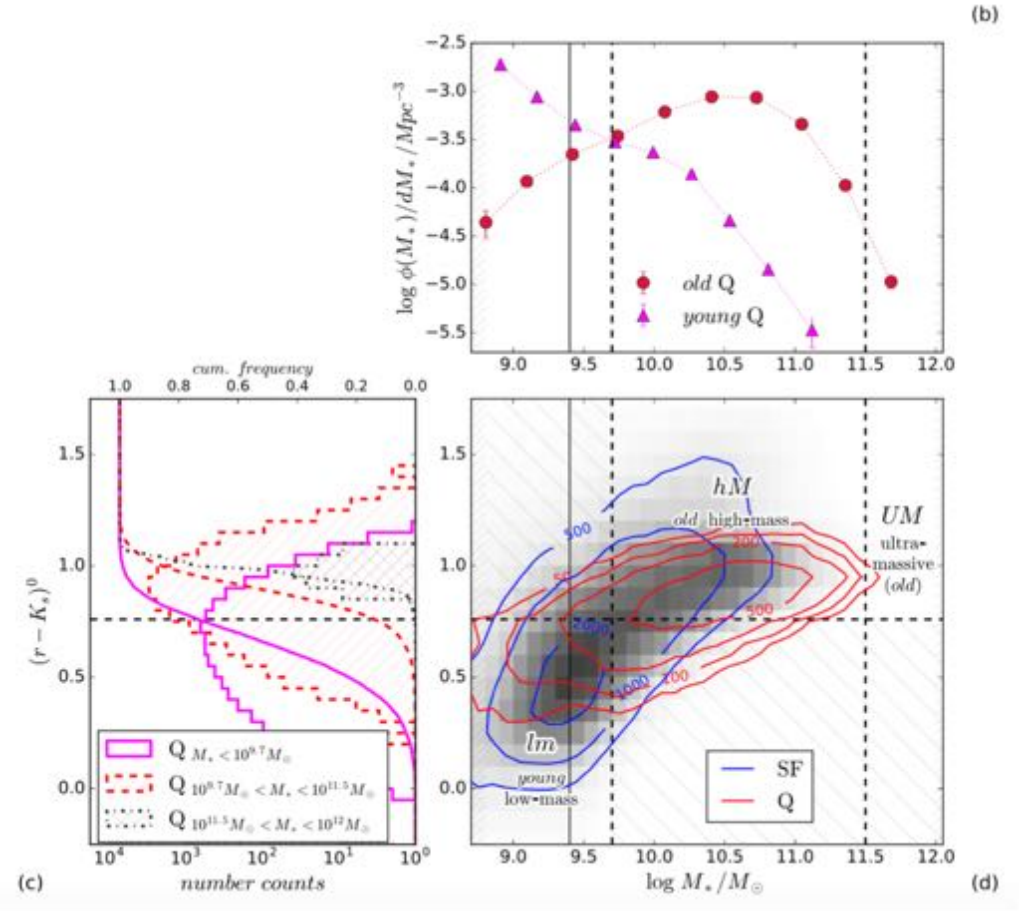

The probability distribution functions of the local density

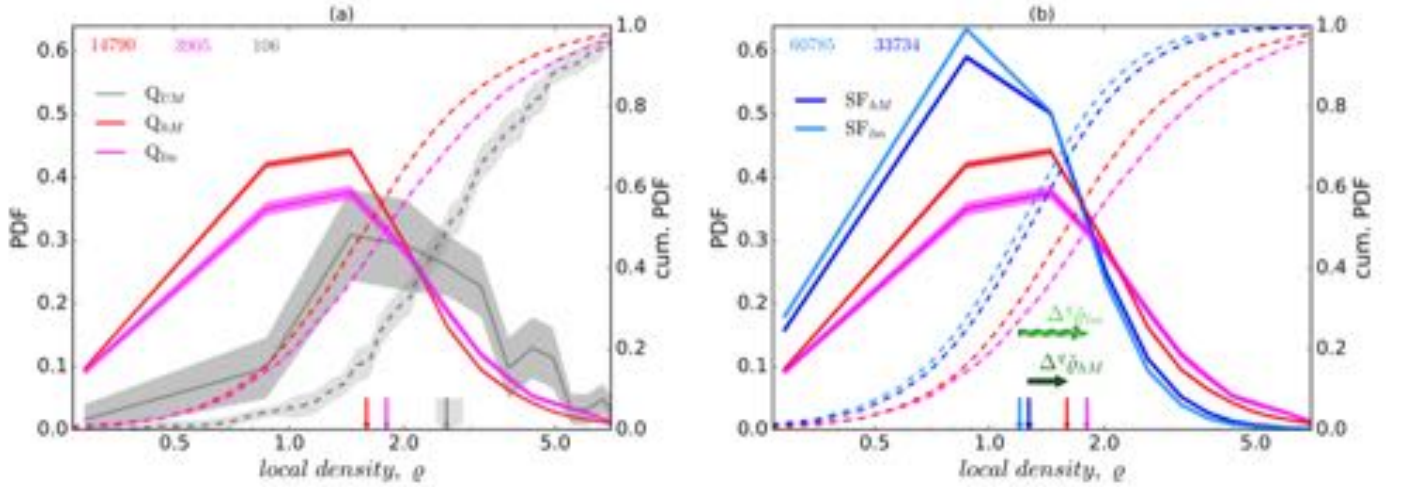

Figure 4. Probability distribution function (PDF) of the local density ϱ, as measured in 0.5 Mpc radius apertures at redshift $0.2 < z < 0.5$ for **(a)** quiescent low-mass (magenta), high-mass (red) and ultra-massive (grey) galaxies and **(b)** comparison with star-forming counterparts for low-mass (cyan), high-mass (blue) galaxies. Dashed lines show the corresponding cumulative PDFs, while vertical arrows show the corresponding typical local densities, $\bar{\varrho}$, defined as PDF medians. Only galaxies with $M_* \geq M_{lim}(z < 0.5) = 10^{9.8} M_\odot$ are considered. Shaded envelops represent the corresponding $\pm 1\sigma$ uncertainties derived from bootstrap resampling, while the galaxy number of each subsample is written in the upper left corner. Horizontal green arrows (in panel b) show the local density deviation associated with the different quenching channels: $\Delta^q\bar{\varrho}_{lm}$ (dashed light green arrows) and $\Delta^q\bar{\varrho}_{hM}$ (dark green arrows) for low-mass galaxies prone to fast quenching and high-mass galaxies prone slow quenching, respectively (cf. Sect. 3.2).

- Quiescent galaxies are located in denser environments than star-forming ones, both for low-mass and high-mass galaxies.
- Low-mass quiescent galaxies are located in denser environments than high-mass ones.
- The quiescence of low-mass galaxies, associated with fast quenching, requires a stronger increase of the local density.

[3] On the (fast) quenching of (young) low-mass galaxies to z~0.6

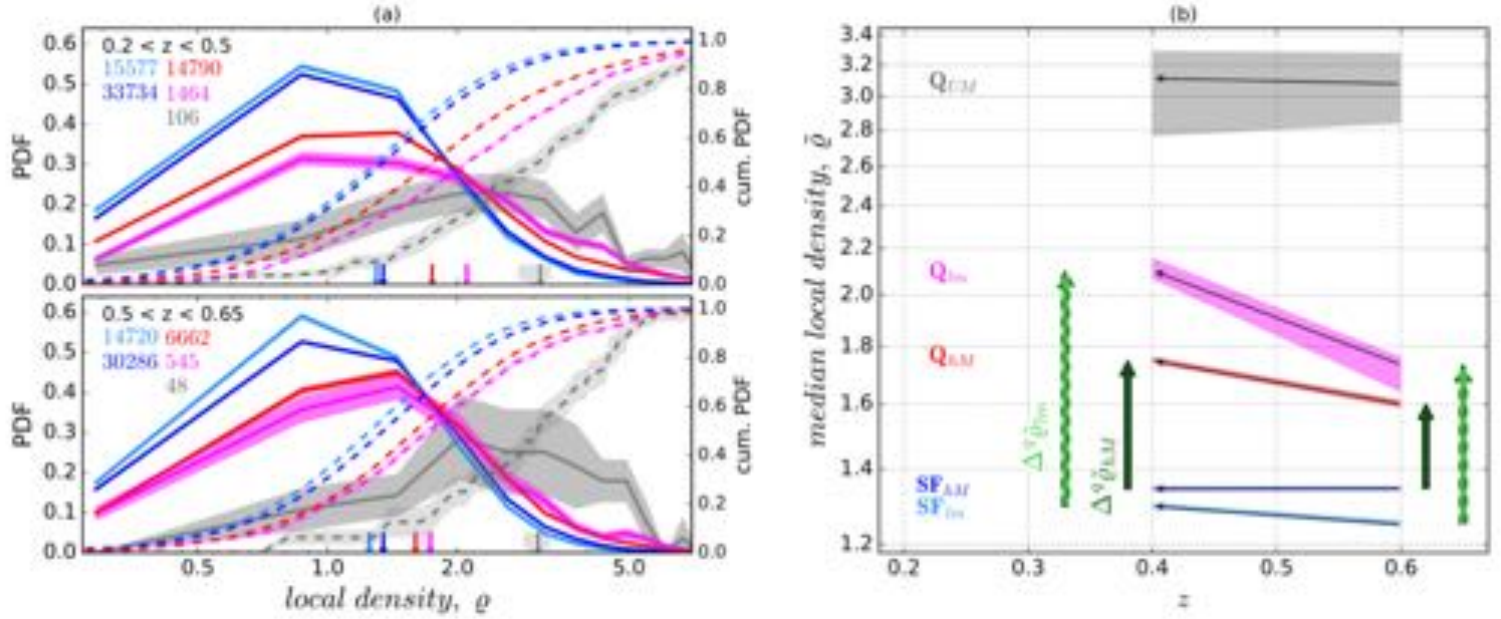

Figure 5. Evolution of local densities with redshift, considering galaxies with $M_\star \geq M_{\lim}(z < 0.65) = 10^{9.4} M_\odot$. **(a)** PDF($\varrho$) (solid lines) and cumulative PDF(ϱ) (dashed lines) at redshift $0.2 < z < 0.5$ (top) and $0.5 < z < 0.65$ (bottom) for the different classes of galaxies defined in Sect. 3.2: low-mass quiescent (Q_{lm}; magenta) and star-forming (SF_{lm}; light blue) galaxies, high-mass quiescent (Q_{hM}; red) and star-forming (SF_{hM}; dark blue) ones and ultra-massive galaxies (Q_{UM}; grey). The galaxy number of each subsample is written in the upper left corner. **(b)** Corresponding evolution of the median local density $\tilde{\varrho}$ (cf. Sect. 4) with redshift between $z \sim 0.6$ and $z \sim 0.4$ (median redshifts of $0.5 < z < 0.65$ and $0.2 < z < 0.5$, respectively). Similarly to Fig. 4, shaded envelopes represent the corresponding $\pm 1\sigma$, as derived from bootstrap resampling. Vertical green arrows show the local density deviation associated with the different quenching channels, at $0.2 < z < 0.5$ and $0.5 < z < 0.65$: $\Delta^q\tilde{\varrho}_{lm}$ (dashed light green arrows) and $\Delta^q\tilde{\varrho}_{hM}$ (dark green arrows) for low-mass galaxies prone to fast quenching and high-mass galaxies prone slow quenching, respectively (cf. Sect. 3.2).

Conclusion : The local overdensity is associated the rapid quenching of low-mass quiescent galaxies, while the physical mechanism is still uncertain.